Journal of Zhejiang University-SCIENCE B (Biomedicine & Biotechnology) 2021 22(2):123-135
www.jzus.zju.edu.cn; www.springer.com/journal/11585
E-mail: jzus_b@zju.edu.cn

Research Article

https://doi.org/10.1631/jzus.B2000540

Check for updates

Modeling the neuro-protection of theaflavic acid from black tea and its synergy with nimodipine via mitochondria apoptotic pathway

Dan MU, Huaguang QIN, Mengjie JIAO, Shaogui HUA, Tingzhe SUN✉

School of Life Sciences, the Province Key Laboratory of the Biodiversity Study and Ecology Conservation in Southwest Anhui, Anqing Normal University, Anqing 246133, China

Abstract: Ischemic stroke presents a leading cause of mortality and morbidity worldwide. Theaflavic acid (TFA) is a theaflavin isolated from black tea that exerts a potentially neuro-protective effect. However, the dynamic properties of TFA-mediated protection remain largely unknown. In the current study, we evaluated the function of TFA in the mitochondria apoptotic pathway using mathematical modeling. We found that TFA-enhanced B-cell lymphoma 2 (Bcl-2) overexpression can theoretically give rise to bistability. The bistability is highly robust against parametric stochasticity while also conferring considerable variability in survival threshold. Stochastic simulations faithfully match the TFA dose response pattern seen in experimental studies. In addition, we identified a dose- and time-dependent synergy between TFA and nimodipine, a clinically used neuro-protective drug. This synergistic effect was enhanced by bistability independent of temporal factors. Precise application of pulsed doses of TFA can also promote survival compared with sustained TFA treatment. These data collectively demonstrate that TFA treatment can give rise to bistability and that synergy between TFA and nimodipine may offer a promising strategy for developing therapeutic neuro-protection against ischemic stroke.

Key words: Theaflavic acid (TFA); Nimodipine; Ischemic stroke; Apoptosis; Synergy

1 Introduction

Ischemic stroke is characterized by induction of inflammatory and hypoxic responses owing to deprivation of glucose and oxygen in the brain (Yang et al., 2019). Apoptosis will be triggered in the penumbra, the area around the ischemic core without restored blood flow, possibly because of massive production of reactive oxygen species (ROS) and reduced adenosine triphosphate (ATP) levels in these tissues (Mehta et al., 2007). However, reperfusion of blood flow will also exacerbate the brain injury via uncontrolled oxidative stress (Thompson et al., 2012). B-cell lymphoma 2 (Bcl-2) family members have been shown to actively participate in ischemia-induced apoptosis (Koubi et al., 2005). Under oxidative stress, overexpression of the anti-apoptotic member Bcl-2 can reduce ROS production below harmful levels and inhibit apoptosis (Seidman et al., 2002, 2004; Chong et al., 2014). Therefore, precise regulation of Bcl-2 expression can exert a cytoprotective effect for brain tissue under oxygen and glucose deprivation/restoration (OGD/R) (Koubi et al., 2005).

Bcl-2 family members contribute significantly to apoptosis and can be categorized into three major classes: anti-apoptotic, pro-apoptotic, and Bcl-2 homology 3 (BH3)-only proteins (Youle and Strasser, 2008). The complex interactions among Bcl-2 family proteins confer bistability and determination of cell fate (Sun et al., 2010; Yin et al., 2017). Recently, Li et al. (2020) identified the role of theaflavic acid (TFA), a phytochemical extracted from black tea, in inhibiting mitochondrial apoptosis in pheochromacytoma 12 (PC12) cells. TFA promotes translocation of the nuclear factor erythroid 2-related factor 2 (Nrf2) into the nucleus and activates anti-oxidant response element (ARE) signaling to up-regulate the expression of anti-apoptotic Bcl-2 proteins (Niture and Jaiswal, 2012; Li et al., 2020). Therefore, TFA may regulate the "Bcl-2 apoptotic switch" (Sun et al., 2010) by adjusting the expression of

✉ Tingzhe SUN, confucian007@126.com
Tingzhe SUN, https://orcid.org/0000-0002-9575-4993

Received Sept. 11, 2020; Revision accepted Nov. 8, 2020;
Crosschecked Dec. 30, 2020

© Zhejiang University Press 2021

anti-apoptotic proteins. Bistability is characterized as a typical switch-like transition between alternative states (Tyson et al., 2003). However, it seems that the protective effect of TFA exhibits a gradient pattern (Li et al., 2020). Therefore, understanding of the dynamics and detailed mechanisms of TFA-mediated cytoprotective effects and of the means by which TFA tips the balance between alternative cell fates remains largely elusive.

Previous studies have demonstrated that TFA can induce Nrf2 nuclear translocation and promote production of Bcl-2 (Niture and Jaiswal, 2012; Li et al., 2020). Furthermore, it is also possible that enhanced production of the anti-apoptotic Bcl-2 induces bistability (Sun et al., 2010). The aim of the current study is to investigate the theoretical possibility of the ability of TFA to potentiate a bistable response in OGD/R. Ordinary differential equations (ODEs) were constructed to delineate the intricate interactions among Bcl-2 family members and TFA. Local sensitivity coefficients were calculated to determine sensitive parameters. Stochastic simulations were performed to evaluate robustness and patterns of bistability. Nimodipine has been identified as a neuroprotective drug (Roine et al., 1990). In the present work, the synergistic effects between TFA and nimodipine treatment in neuroprotection were also evaluated. Bliss and Loewe combination indexes were used to quantify the synergy.

2 Materials and methods

2.1 Model construction

We have previously constructed a model that describes the mitochondrial apoptotic pathway, with two independent positive feedback loops (the complex interactions among Bcl-2 family members and Bcl-2-associated X/Bcl-2 antagonist/killer (Bax/Bak) autoactivation); this model displays bistable responses in the levels of Bcl-2 family members (Sun et al., 2010). Bcl-2 family members contribute significantly to intrinsic apoptosis (Legrand et al., 2019). Briefly, the pro-apoptotic proteins include Bax group proteins (e.g., Bax, Bak, or Bcl-2-related ovarian killer (Bok)) and BH3-only members (e.g., BH3-interacting domain death agonist (Bid), Bcl-2-associated agonist of cell death (Bad), Bcl-2-like 11 (Bim), Bcl-2-modifying factor (Bmf), p53-up-regulated modulator of apoptosis (Puma), and nicotinamide adenine dinucleotide phosphate (NADPH) oxidase heavy chain subunit A (Noxa)), which contain only the BH3-only domain (Legrand et al., 2019). The anti-apoptotic members comprise Bcl-2 and B-cell lymphoma-extra large (Bcl-x_L) (Legrand et al., 2019). In response to damage signals, Bax monomers and BH3-only members can translocate from the cytosol to the mitochondrial outer membrane (MOM) and relocation of Bcl-2 family members can be viewed as the initial phase of MOM permeabilization (MOMP) and apoptosis (Tsujimoto, 2003). Selected members of BH3-only proteins are "activators," which enable conformational change and Bax/Bak (hereafter dubbed "Bax" for simplicity) pore formation, whereas other BH3-only members are designated as "enablers" by competitive interaction with anti-apoptotic members (Letai et al., 2002). Anti-apoptotic members (labeled "Bcl-2" for simplicity) can serve as inhibitors to counteract the effects of proapoptotic proteins (Letai et al., 2002). Activated Bax/Bak monomers can aggregate and induce formation of the mitochondrial apoptosis channel (MAC) (Dejean et al., 2005). Numerous pro-apoptotic signals can trigger apoptosis by modulating expression of anti- and pro-apoptotic Bcl-2 family members (Willis and Adams, 2005); therefore, we considered the production rate of diverse Bcl-2 family members instead of cytotoxic stress as bifurcation parameters as previously described (Cui et al., 2008). We only considered the effect of Bcl-2 family members on apoptosis; non-canonical functions (e.g., autophagy, inflammation, and senescence) which indirectly affect apoptosis (Chong et al., 2020) were not considered in this study.

In our model, we aimed to investigate the effects of TFA from black tea using mathematical modeling (Li et al., 2020). Li et al. (2020) found that TFA can protect PC12 cells from apoptosis induced by OGD/R. Mechanistic study has suggested that TFA up-regulates the expression of an antiapoptotic Bcl-2 protein by promoting the nuclear translocation of Nrf2 and ARE signaling (Li et al., 2020). Indeed, Nrf2 can bind the *Bcl-2* ARE and induce *Bcl-2* gene expression under stressed conditions (Niture and Jaiswal, 2012). Therefore, we assumed that total Nrf2 centration is constant (Liu et al., 2017) and TFA can increase the nuclear fraction of Nrf2 (Table S1) (Li et al., 2020). Mathematically, $\mathrm{Nrf2}_{nuc}=[k_{basal}+(1-k_{basal})\times \mathrm{TFA}\times k_{in}/(\mathrm{TFA}\times k_{in}+k_{out})]\times \mathrm{Nrf2}_T$, where $\mathrm{Nrf2}_{nuc}$ is the nuclear Nrf2 concentration, $\mathrm{Nrf2}_T$ is the total Nrf2 concentration,

k_{in} and k_{out} characterize the nuclear import and export of Nrf2 induced by TFA, respectively, and the parameter k_{basal} represents the basal nuclear Nrf2 fraction according to the experiments of Li et al. (2020) (i.e., under OGD/R without TFA treatment in PC12 cells, there exists a significant nuclear Nrf2 fraction). Promoter activity of *Bcl-2* ARE was then expressed as $Nrf2_{nuc}/(Nrf2_{nuc}+K_{Nrf2})$, where K_{Nrf2} is the threshold concentration for $Nrf2_{nuc}$. Parameters K_{Nrf2}, k_{basal}, k_{in}, and k_{out} were fitted to the TFA dose response for transcriptional activity of ARE-bound Nrf2 from the experiments of Li et al. (2020) (Fig. 1f). Transcriptional induction of Bcl-2 by nuclear Nrf2 was modeled as $p_{Bcl\text{-}2}=p_{TFA}\times Nrf2_{nuc}/(Nrf2_{nuc}+K_{Nrf2})$, where p represents production (Tables S1 and S2).

To evaluate the potential synergistic effects of TFA and nimodipine co-treatment, the regulatory role of nimodipine was incorporated into our model. Liu et al. (2004) found that nimodipine can up-regulate *Bcl-2* messenger RNA (mRNA) expression while down-regulating *Bax* mRNA; thus, nimodipine can affect the production of both Bcl-2 and Bax proteins. To reflect our assumption that nimodipine increases the production rate of Bcl-2, we introduced an additional term for Bcl-2 production (Table S1). In the model with TFA and nimodipine co-treatment,

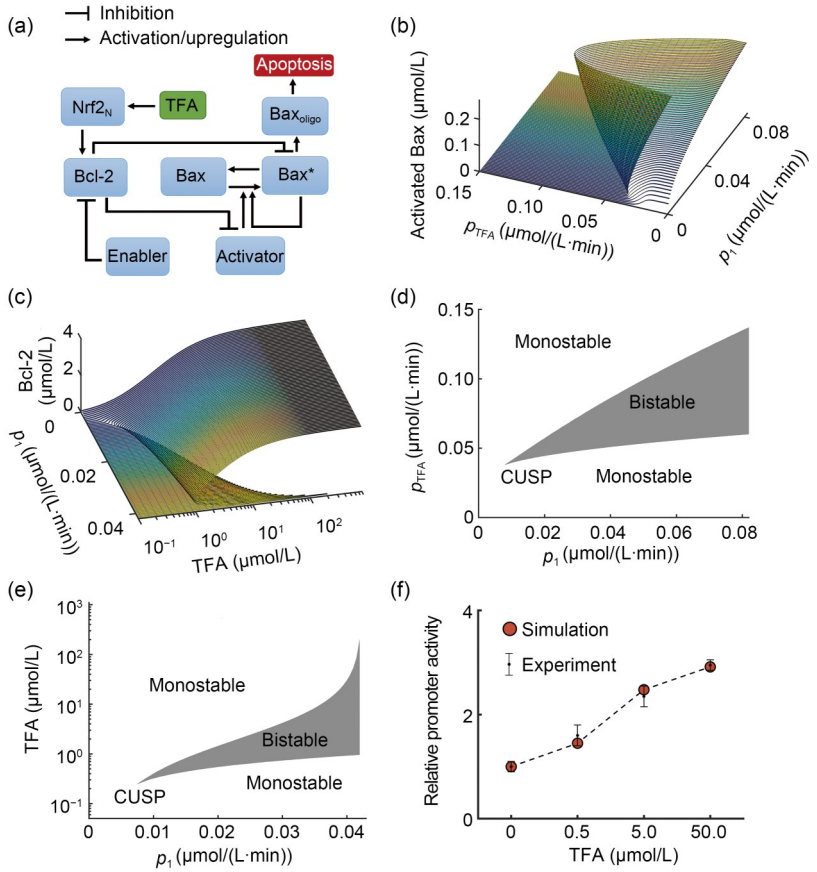

Fig. 1 Bistability of B-cell lymphoma 2 (Bcl-2) family interaction network under theaflavic acid (TFA) treatment. (a) Schematic diagram of current model. TFA promotes translocation of nuclear factor erythroid 2-related factor 2 (Nrf2) into nucleus ($Nrf2_N$) to activate anti-oxidant response element (ARE) signaling. Nuclear Nrf2 can induce Bcl-2 expression. Bax^* is the activated Bcl-2-associated X (Bax). (b) Two-parameter bifurcation diagram for activated Bax. Bax production rate (p_1) and maximal Bcl-2 production rate by TFA treatment (p_{TFA}) were used as bifurcation parameters. The folded area indicates the bistable region. (c) Two-parameter bifurcation diagram for Bcl-2 using p_1 and TFA as bifurcation parameters. (d) Bistable region is shown as shaded area, which represents the folded area for (b). CUSP bifurcation is indicated. (e) Bistable domain is represented as shaded area, which represents the folded area for (c). (f) TFA dose response for relative *Bcl-2* promoter activity. The error bars were adopted from the study of Li et al. (2020). The red dots were obtained from model simulation. The promoter activity in our model denotes $p_{Bcl\text{-}2}=p_{TFA}\times Nrf2_{nuc}/(Nrf2_{nuc}+K_{Nrf2})$, where $Nrf2_{nuc}$ is the nuclear Nrf2 concentration, K_{Nrf2} is the threshold concentration for $Nrf2_{nuc}$, and p represents production (Tables S1–S3).

$p_{\text{Bcl-2}}$ was modified as: $p_{\text{Bcl-2}}=p_{\text{TFA}}\times\text{Nrf2}_{\text{nuc}}/(\text{Nrf2}_{\text{nuc}}+K_{\text{Nrf2}})+p_{\text{Nimo}}\times\text{Nimo}/(Ec+\text{Nimo})$, where Nimo denotes the concentration of nimodipine and Ec is the threshold concentration for nimodipine. The term $p_{\text{Nimo}}\times\text{Nimo}/(Ec+\text{Nimo})$ represents the effect of nimodipine-enhanced Bcl-2 production. In addition, the Bax production rate p_1 was further modified as p_1', in which $p_1'=p_1\times Ec/(Ec+\text{Nimo})$. This term characterizes the effect of nimodipine-induced Bax suppression. For simplicity, we assumed that enhancement of Bcl-2 production and inhibition of Bax production had an identical threshold value Ec. Since treatment of PC12 cells with 50 μmol/L nimodipine alone had similar effects as in cells treated with 50 μmol/L TFA (Li et al., 2020), the Ec value was estimated to yield temporal profiles in dynamics of cells treated with 50 μmol/L TFA.

All kinetic interactions were formulated using ODEs (Tables S1 and S2) and parameter values are shown in Table S3. Parameter values for the Bcl-2 activation switch (k_1 to k_{17}, u_1 to u_9, p_1 and p_3) were assigned based on our previous work (Sun et al., 2009).

2.2 Stochastic simulation

Stochastic simulations were implemented using the Poisson τ-leap method to characterize intrinsic noise and improve computational efficiency in well-stirred systems (Tian and Burrage, 2006). Briefly, suppose that there are N species in the system [S_1, S_2, ⋯, S_N] with molecular number $\boldsymbol{x}=X_i(t)$ for species S_i at time t. These species interact dynamically with each other via reaction channels [R_1, R_2, ⋯, R_M]. For R_j, the propensity function $a_j(\boldsymbol{x})$ for a given state inside a volume Ω. Therefore, $a_j\mathrm{d}t$ denotes the probability of occurrence for reaction R_j, in the infinitesimal time interval [t, $t+\mathrm{d}t$). The element v_{ij} state vector $\boldsymbol{v}_j$ represents the change in molecular numbers for species S_i owing to the reaction R_j.

In the Poisson τ-leap method, the number (M) of reactions for channel R_j firing at time interval [t, $t+\tau$) obeys Poisson distribution (P) with mean $a_j\tau$. The system is updated following the rule:

$$x(t+\tau)=x(t)+\sum_{j=1}^{M}\boldsymbol{v}_j P(a_j(\boldsymbol{x})\tau).$$

Extrinsic noise was also incorporated by perturbing the parameters by multiplying them with lognormally distributed random variables (μ=1, σ^2=0.02) (Keizer et al., 2019). Therefore, in our stochastic simulations, both intrinsic noise and extrinsic noise were considered.

2.3 Bifurcation analysis

Bifurcation data were obtained using the MATLAB package MATCONT (Dhooge et al., 2003).

2.4 Synergy

Synergy was evaluated using the Loewe and Bliss combination indices (CIs) (Straetemans et al., 2005; Fitzgerald et al., 2006). The Loewe combination index CI_{Loewe} is defined as follows:

$$\text{CI}_{\text{Loewe}}=\frac{d_1}{C_x^{(1)}}+\frac{d_2}{C_x^{(2)}},$$

where d_1 (TFA) and d_2 (nimodipine) are the agent doses in the combination isobologram with respect to x (10% or 40%) percentage decrease in total levels of activated Bax, $C_x^{(1)}$ and $C_x^{(2)}$ denote the concentrations of a single TFA and nimodipine dose, respectively, leading to x (10% or 40%) percentage decrease in total levels of activated Bax. $\text{CI}_{\text{Loewe}}<1$, $\text{CI}_{\text{Loewe}}=1$, and $\text{CI}_{\text{Loewe}}>1$ indicate Loewe synergy, additivity, and antagonism, respectively.

The Bliss independence or combination index CI_{Bliss} is defined as:

$$\text{CI}_{\text{Bliss}}(x,y)=\frac{R_1(x)+R_2(y)-R_1(x)R_2(y)}{R_{12}(x,y)},$$

where $R_1(x)$, $R_2(y)$, and $R_{12}(x, y)$ denote the relative changes in total levels of activated Bax to TFA (at a dose of x), nimodipine (at a dose of y), and TFA-nimodipine combination treatment (at a dose combination of [x, y]), respectively. As a result, $\text{CI}_{\text{Bliss}}<1$, $\text{CI}_{\text{Bliss}}=1$, and $\text{CI}_{\text{Bliss}}>1$ indicate synergistic, additive, and antagonistic effects, respectively.

2.5 Local sensitivity coefficient

Local sensitivity can evaluate the dynamic responses to infinitesimal changes in kinetic parameters. A dynamic system can be defined by $\boldsymbol{x}'=f(\boldsymbol{x},\boldsymbol{\theta})$, where $\boldsymbol{x}$ and $\boldsymbol{\theta}$ represent the state and parameter vectors, respectively. Local sensitivity coefficient $\boldsymbol{S}$ is defined by

$$\boldsymbol{S}=\frac{\partial \text{SN}_i/\text{SN}_i}{\partial\boldsymbol{\theta}/\boldsymbol{\theta}}=\frac{\partial\ln\text{SN}_i}{\partial\ln\boldsymbol{\theta}},$$

where SN_i (i=1 or 2) is the saddle node in bifurcation diagram.

2.6 Model simulation

The integration of ODEs and numerical simulations was performed using MATLAB (R2018b).

3 Results

3.1 Potential bistability induced by TFA-enhanced Bcl-2 production

TFA can accelerate production of Bcl-2 via increased Nrf2 nuclear translocation (Li et al., 2020). We incorporated this effect into our model of Bax activation switch (see Section 2; Fig. 1). After OGD/R, excess ROS will lead to mitochondrial damage and induce apoptosis in neuronal cells (Luo et al., 2013; Li et al., 2020). Therefore, the initial state of cells after OGD/R should be a pro-apoptotic state with high level of activated Bax or low levels of anti-apoptotic proteins. After TFA treatment, expression of anti-apoptotic Bcl-2 is reinforced and cells may revert to a survival state if overexpressed Bcl-2 can effectively antagonize pro-apoptotic proteins (e.g., Bax) (Figs. S1a–S1d). We observed that the system displayed bistability characterized by the folded region in the two-parameter bifurcation diagram (Fig. 1b). As the Bax production rate (p_1) increased, we noted that a higher TFA-induced Bcl-2 production rate (p_{TFA}) was required to "neutralize" activated Bax and maintain a state with extremely low levels of the pro-apoptotic Bax proteins (i.e., survival state; Fig. 1b). As expected, higher doses of TFA were needed when p_1 was elevated to maintain high levels of Bcl-2 and cellular survival (Fig. 1c). We could identify CUSP bifurcation points in the two-parameter bifurcation diagrams and the bistable regions were enlarged at higher p_1 (Figs. 1d and 1e). We also noted that the simulated dose response of TFA for Bcl-2 promoter activity was consistent with the findings of Li et al. (2020) (Fig. 1f). These results suggest that TFA treatment may reshape the bistability of the intrinsic apoptotic pathway.

3.2 Sensitivity analysis for bistability

We then evaluated parametric sensitivity for bistable responses. When p_{TFA} is significantly increased, Bcl-2 overexpression may effectively counteract activated Bax (Fig. 2a). In the bifurcation diagram for activated Bax with reference to p_{TFA}, two saddle nodes (SN_1 and SN_2) can be identified and SN_2 indicates a deterministic threshold for survival after OGD/R (Fig. 2a). Not surprisingly, p_1 positively affected both saddle nodes (Figs. 1b and 2b). Production rate of pro-apoptotic BH3-only proteins also markedly increased the threshold for survival (Fig. 2b). As expected, the degradation rates for inactive Bax and BH3-only members played a negative role (Fig. 2b). Two parameters k_{basal} and k_{Nrf2} showed the highest sensitivities for SN_1 and SN_2, respectively, since they were directly associated with Bcl-2 production (Fig. 2b). Notably, activator (u_3) and MAC (u_9) degradation rates specifically lowered the threshold for survival (SN_2) (blue bars, Fig. 2b). From sensitivity analysis, we could identify universal and specific factors to regulate cellular threshold for survival and death.

3.3 Robustness features of TFA-mediated bistability

Since TFA-induced bistability is an important contributor to cellular survival after OGD/R, we further investigated the property of robustness. From bifurcation theory, the steady state connecting SN_1 and SN_2 is unstable (Tyson et al., 2003). Once a "cell" overcomes the barrier height between the unstable steady state and the higher (upper) steady state for activated Bax after OGD/R, the lower steady state will be reached and a "cell" will survive within the bistable region (Fig. 3a). We defined the maximal barrier height as the largest difference in activated Bax levels between the high and unstable steady state (Fig. 3a). First, we varied all parameters around their reference values by multiplying them with a lognormally distributed random variable (i.e., μ=1, σ^2=0.1, 0.2, or 0.3). Interestingly, we noted that TFA-induced bistability was highly robust and more than 90% of simulations retained bistability even when the variance reached 0.3 (90.1%, Fig. 3b). Under parametric stochasticity, we noted that SN_1 was relatively less variable, while SN_2 showed higher variation (Fig. 3c). Notably, TFA induces Bcl-2 expression; once the productive effect of Bcl-2 exceeds the SN_2 threshold, the levels of active Bax will dramatically decrease and cells may revert to a survival state after OGD/R (Fig. 2a). Therefore, a highly variable SN_2 implies that the transition between alternative cell fates (survival and death) might frequently occur after TFA treatment. Importantly, we found only a minimal correlation between maximal

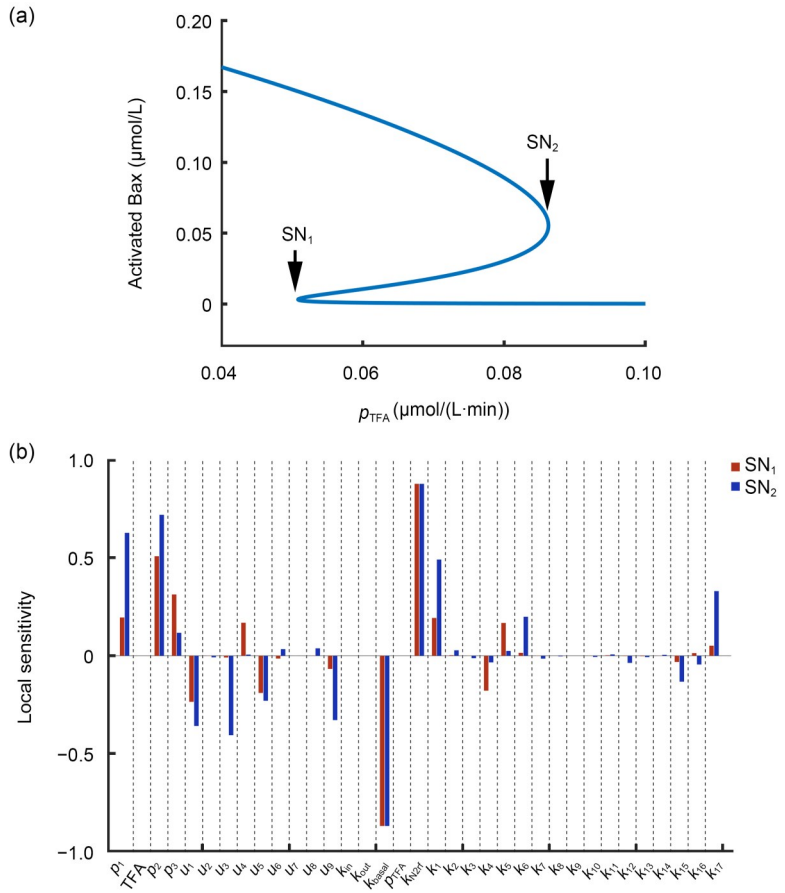

Fig. 2 Sensitivity analysis for bistable switch. (a) Bifurcation diagram for activated B-cell lymphoma 2 (Bcl-2)-associated X (Bax) using theaflavic acid (TFA)-induced Bcl-2 production rate (p_{TFA}) as bifurcation parameter. The saddle node (SN) points are indicated (SN_1 and SN_2). SN_2 represents the threshold for the survival state under oxygen and glucose deprivation/restoration (OGD/R). (b) Local parameter sensitivity for SN_1 (red) and SN_2 (blue) was evaluated with TFA of 0 μmol/L.

barrier height and SN_1 (Fig. 3d, left), but a strong correlation between maximal barrier height and SN_2 (Fig. 3d, middle). The correlation was further improved if the bistable range (SN_2−SN_1) was used as the metric (Fig. 3d, right). Taken together, although the bistability is robust, the threshold for survival is highly variable.

3.4 TFA dose-dependent responses via stochastic simulations

We then performed stochastic simulations to evaluate TFA dose-dependent responses. Under 5 μmol/L TFA treatment, stochastic simulations identified that specific runs retained high levels of activated Bax, whereas some runs led to collapse in levels of activated Bax (Fig. 4a). If "cells" could revert to survival state after OGD/R, we then evaluated their recovery rate by measuring the half recovery time (Figs. 4a and 4b). We found that increasing TFA doses accelerated recovery and survival (Fig. 4b). Average half recovery time changed from 3.40, 3.18 to 2.92 h as the TFA dose increased from 5, 10 to 50 μmol/L (Fig. 4b). Not surprisingly, higher TFA doses decreased the average levels of activated Bax while raising levels of Bcl-2 (Fig. 4c), thus qualitatively aligning with experimental data (Li et al., 2020). Li et al. (2020) found that about (48.9±5.1)% of PC12 cells are viable when treated without TFA after OGD/R, and treatment with TFA dosages may increase the percentage of viable cells. Our stochastic simulations assumed a hypothetical threshold of activated Bax which differentiates survival from death (Fig. 4d, dashed lines). Varying the threshold level of activated Bax yielded a final viability fraction from 43.8% (i.e., 48.9%−5.1%) to 54.0% (i.e., 48.9%+5.1%); we evaluated whether our simulations matched the experimentally determined dose response of TFA (Li et al., 2020). When the threshold

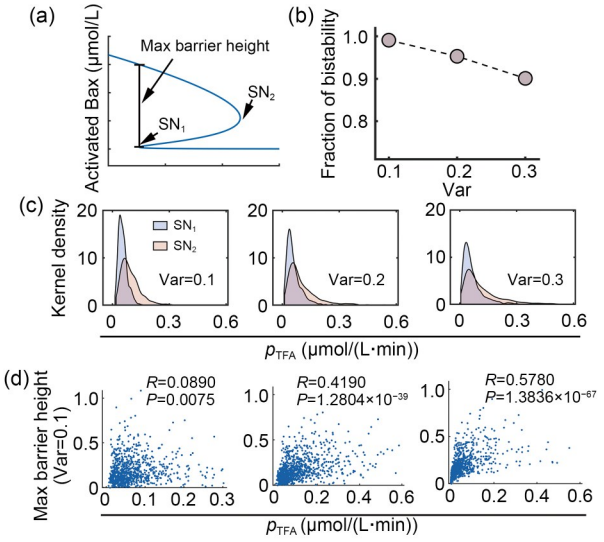

Fig. 3 Robustness analysis for bistability. (a) Example of bistability in activated B-cell lymphoma 2 (Bcl-2)-associated X (Bax). The maximal (max) barrier height indicates the largest barrier a cell needs to overcome for survival. The two saddle nodes (SN_1 and SN_2) are indicated. (b) Fraction of bistability by simultaneous parameter variation. All parameters were randomized around the reference values by multiplying with a lognormally distributed random variable (μ=1, σ^2=0.1, 0.2, or 0.3 as indicated). One thousand simulations were run for each variance. (c) Dispersion of SN_1 and SN_2 under simultaneous parameter variation. From left to right, variance (Var)=0.1, 0.2, and 0.3. The coefficient of variation (CV): SN_1=0.4394, SN_2=0.5434 (left); SN_1=0.6699, SN_2=0.8283 (middle); SN_1=0.8834, SN_2=1.0010 (right). (d) Correlation between maximal barrier height and SN_1 (left), SN_2 (middle), or bistable range (SN_2–SN_1, right). σ^2=0.1. p_{TFA}: theaflavic acid (TFA)-induced Bcl-2 production rate.

is defined as indicated (46.9% viability; Fig. 4d, top), the TFA dose response most closely matches the experimental data (Li et al., 2020). However, consistency was identified after a 4-h TFA treatment (Figs. 4d (top) and 4e), which is in accordance with the experimental setting by Li et al. (2020) (viability in their experiments was measured after 4 h TFA treatment). When viability was evaluated for a 12-h TFA treatment after OGD/R, the deviation in simulated TFA dose responses from experimental data was significant (Figs. 4d (bottom) and 4f). Notably, the bimodal response, which is a notable characteristic of bistability (Tyson et al., 2003), could be observed at later time points (e.g., 12 h TFA treatment; Fig. 4d, bottom). These results suggested that the TFA dose response is time-dependent and bimodality can be detected only at later time points.

3.5 Optimal modulation of synergistic responses between TFA and nimodipine

Previous work has shown that the neuro-protective drug nimodipine can up-regulate Bcl-2 expression while simultaneously inhibiting Bax expression (Liu et al., 2004). Applying nimodipine to PC12 cells, Li et al. (2020) also found that 50 μmol/L nimodipine has an effect similar to that of 50 μmol/L TFA in viability and apoptosis assays. We then incorporated the effect of nimodipine in our model (see Section 2; Fig. S2) to investigate the potential synergy for combined TFA-nimodipine treatment. We found that nimodipine treatment could give rise to systematic bistability (Fig. 5a). The two-parameter bifurcation diagram also shows that specific combinations of TFA and nimodipine guaranteed bistable responses (Fig. 5b, grey). We then examined whether TFA and nimodipine could function cooperatively during recovery from OGD/R using the Bliss combination index (see Section 2). Evaluating the responses for reduction in active Bax monomer (indicative of transition from death to survival) at 4 or 12 h after TFA and nimodipine co-treatment, we found that at 4 h, combined TFA-nimodipine treatment usually had synergistic effects (Fig. 5c). Bistable regions in the two-parameter diagrams indeed increased synergy (Figs. 5c and 5d). At 12 h after TFA-nimodipine co-treatment, however, we could observe both synergy (CI_{Bliss}<1) and antagonism (CI_{Bliss}>1) depending on the doses of TFA and nimodipine (Fig. 5d). Indeed, the regions of highest synergy roughly coincided with the bistable regions (Figs. 5b and 5d). We also analyzed the isobologram of apoptotic responses after combined TFA-nimodipine treatment using the Loewe combination index. Isobolograms (10% and 40%) were evaluated (Fig. 5e). Simulations demonstrated that TFA and nimodipine displayed differential synergistic effects for different conditions. Specifically, TFA and nimodipine showed slight synergy or near-additivity (10%; Fig. 5e, left two panels). However, TFA and nimodipine exhibited remarkable synergy in 40% isobologram (Fig. 5e, right two panels). These data suggest that TFA and nimodipine show objective- and dose-dependent synergism during anti-apoptotic responses.

3.6 Evaluation of impulse responses for TFA

Li et al. (2020) used a continuous TFA dosage to treat PC12 cells; we further extended their findings and evaluated the response to pulsed doses of TFA. Pulses

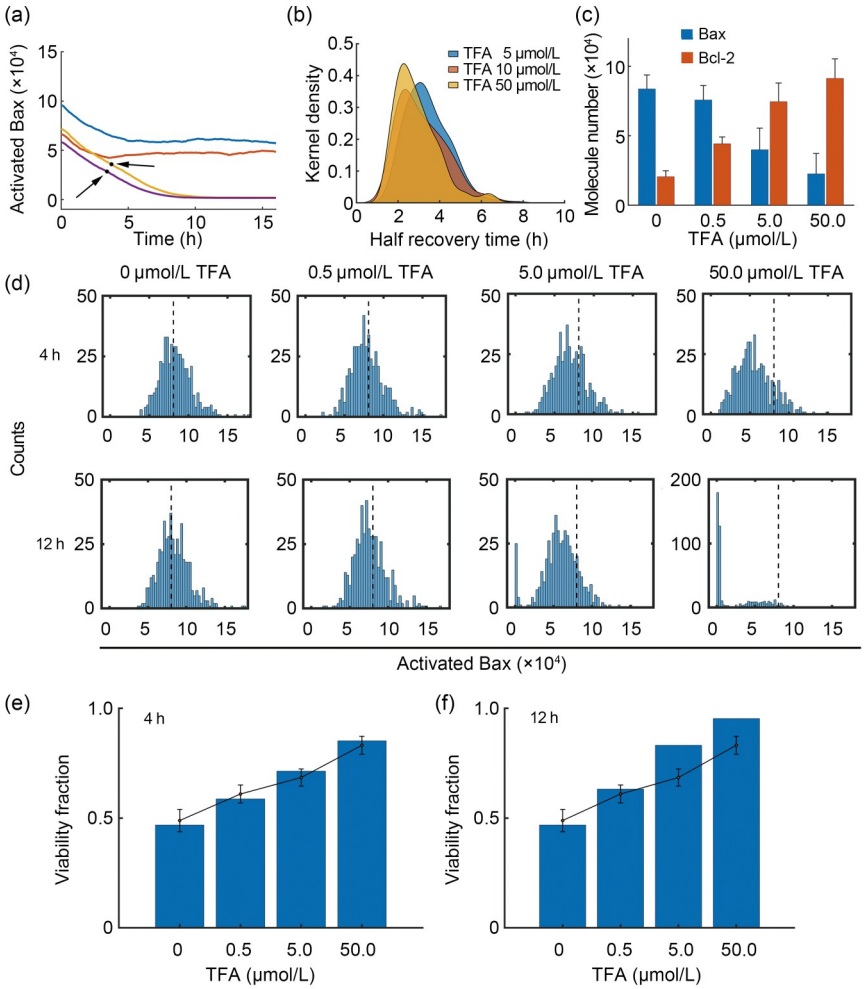

Fig. 4 Stochastic simulation-matched experimental data. (a) Selected stochastic trajectories were treated with 5 μmol/L theaflavic acid (TFA). (b) Distribution of half recovery time for cells treated with 5, 10, or 50 μmol/L TFA. Five hundred stochastic simulations were performed for each TFA dose. Half recovery time is defined as the time at which a stochastic simulation for activated B-cell lymphoma 2 (Bcl-2)-associated X (Bax) reaches half of its initial value and a "cell" commits to survival. The black dots in (a) represent the half recovery time. (c) Total levels of Bcl-2 and Bax in 500 simulations with TFA concentrations of 0, 0.5, 5.0, or 50.0 μmol/L. (d) Distribution of activated Bax in 500 simulations with TFA concentrations of 0, 0.5, 5.0, or 50.0 μmol/L treatments at 4 h (top) or 12 h (bottom). The dashed line denotes the hypothetical threshold for survival derived from experimental data (Li et al., 2020). (e) Fraction of viable cells or simulations after TFA treatment for 4 h. The bars denote simulations, while error bars indicate experimental data (mean±standard deviation, *n*=3). Statistical results for panel (d), top. (f) Similar to (e) after TFA treatment for 12 h. Statistical results for panel (d), bottom.

were reshaped with different durations and terminal heights (the maximum was fixed as 50 μmol/L; Fig. 6a). Note that we applied a super-threshold TFA dose 50 μmol/L (Fig. S1) as the pulse height. However, if the pulse duration did not persist for a sufficiently long time, the level of active Bax monomer could not overcome the threshold and would be maintained at high levels (Fig. 6b). If the duration was longer, however, we observed that Bax dropped to low levels and the cell would commit to survival (Fig. 6c). We further measured the steady state of active Bax monomers and the levels of active Bax at 4 or 12 h after termination of TFA impulse with varying impulse duration and terminal height. We identified a gradual response surface if measurement was performed at 4 h after termination of TFA impulse (Fig. 6d, left). However, a "switch-like" response pattern could be observed when we quantified active Bax monomers at 12 h (Fig. 6d, center). If TFA terminal height was slightly more than 10 μmol/L, even a TFA pulse of small duration would lead to strongly decreased active Bax levels (Fig. 6d, center). A definite "switch-like"

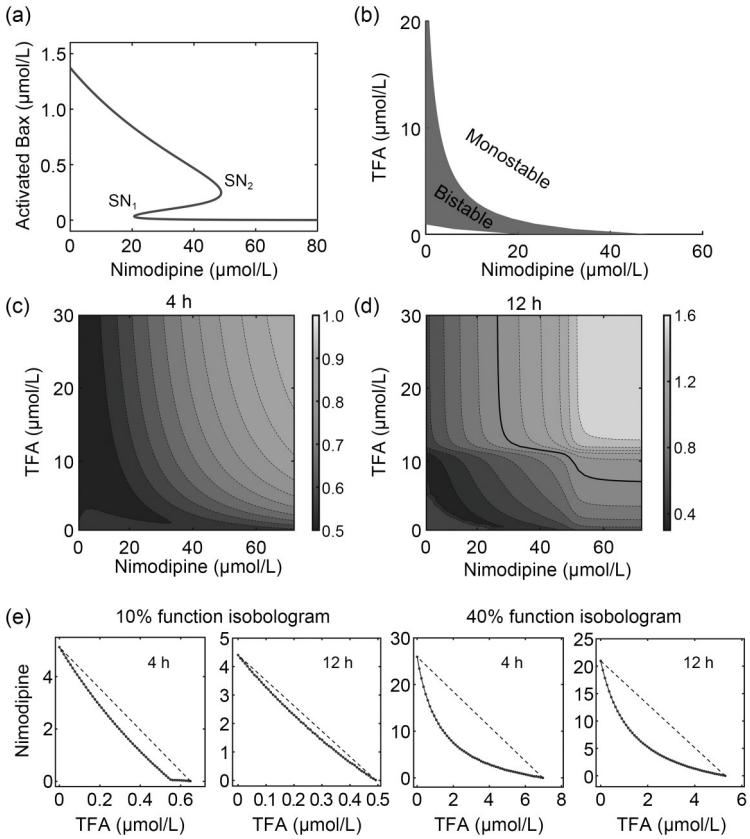

Fig. 5 Synergy between theaflavic acid (TFA) and nimodipine. (a) Bifurcation diagram of activated B-cell lymphoma 2 (Bcl-2)-associated X (Bax) against nimodipine dosage. (b) Bistable region in co-dimension 2 bifurcation diagram. TFA and nimodipine doses are shown. (c) Synergy of the TFA-nimodipine combination was quantified with the Bliss combination index (CI_{Bliss}) when the combinatorial effects were evaluated 4 h after TFA-nimodipine co-treatment. (d) Similar settings to (c), but 12 h after TFA-nimodipine co-treatment. The curve for CI_{Bliss}=1 is highlighted in bold. (e) Isobologram synergy for TFA-nimodipine treatment: 10% (left) and 40% (right) function isobolograms at 4 or 12 h after TFA treatment are shown. Decrease in activated Bax was used as the metric. If the isobologram bowed inward, combined TFA-nimodipine treatment exhibited synergy.

pattern was seen if the steady states were evaluated (Fig. 6d, right). A duration of TFA pulse of more than approximately 400 min would irreversibly cut down active Bax expression irrespective of terminal height (Fig. 6d, right). Similarly, a minor 50 μmol/L TFA pulse with a terminal height of approximately 11.5 μmol/L would always lead to survival (Fig. 6d, right). Collectively, these results demonstrate that appropriate application of TFA pulses can tip the balance between survival and death.

4 Discussion

Since ischemic stroke remains a major threat to health worldwide, this study modeled the impact of TFA on protection of OGD/R-induced apoptosis (Li et al., 2015). We investigated a potential mechanism involving the mitochondria apoptotic pathway. Bistability, which arises from complex interactions in the apoptotic pathway, has been identified in numerous studies (Bagci et al., 2006; Legewie et al., 2006; Chen et al., 2007; Albeck et al., 2008; Cui et al., 2008; Ho and Harrington, 2010; Sun et al., 2010; Yin et al., 2017). TFA, a theaflavin previously isolated from black tea (Li et al., 2020), has been shown to promote translocation of Nrf2 into the nucleus and to activate ARE signaling to increase Bcl-2 expression (Niture and Jaiswal, 2012). Therefore, TFA can regulate the expression of anti-apoptotic proteins and modulate bistability in the apoptotic switch. The modulatory role of TFA is reminiscent of resveratrol-induced apoptosis (Jiang et al., 2005) and suggests that the apoptotic switch can be regulated.

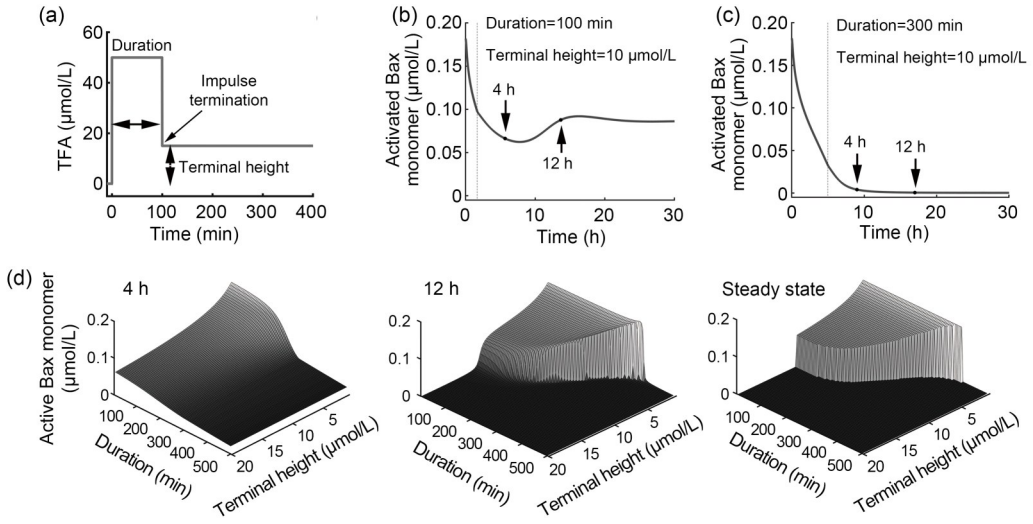

Fig. 6 Impulse response of theaflavic acid (TFA). (a) Sample TFA pulse with defined duration and terminal height. (b, c) Selected TFA pulse responses. TFA was introduced at time point 0 (i. e., immediately after oxygen and glucose deprivation/restoration (OGD/R)) and tested for varying time durations. The dashed lines indicate the end of the TFA pulse. After TFA pulse, TFA dose was maintained at "terminal height" as in (a). The temporal responses for active B-cell lymphoma 2 (Bcl-2)-associated X (Bax) monomer at 4 or 12 h after the TFA impulse termination (i.e., 4 or 12 h behind the dashed lines) as well as the steady state responses were quantified. (d) Levels of active Bax monomers at 4 h (left) or 12 h (center) after the TFA impulse termination and steady state response (right) were evaluated with different combinations of durations and terminal heights.

The ischemic core cannot access sufficient ATP and oxygen because of occlusion of blood flow in cerebral tissues (Pellegrini-Giampietro et al., 2009). Following ischemia and restoration of blood flow, oxygen supply is largely restored, leading to overproduction of ROS and oxidative stress (Saito et al., 2005). The deleterious effects of excessive ROS include activation of the mitochondrial apoptotic pathway and cell death after cerebral ischemia and reperfusion (Chong et al., 2014). Excess ROS can also enhance deletion of mitochondrial DNA and induce hearing loss (Seidman, 2000; Seidman et al., 2000; Coling et al., 2003). The anti-apoptotic member Bcl-2 proteins have a defined role in restraining mitochondria ROS overproduction by facilitating the mitochondrial incorporation of glutathione under oxidative stress (Chong et al., 2014). Therefore, the protective function of TFA in reducing ROS after OGD/R can be mediated by TFA-induced Bcl-2 overexpression (Chong et al., 2014; Li et al., 2020). For the sake of simplicity, we did not incorporate ROS or calcium signaling in our model, since Bcl-2 expression may inversely reflect the intrinsic ROS levels; there is also well-characterized positive crosstalk between ROS and calcium signaling (Görlach et al., 2015). Model fitting to some experimental data reported by Li et al. (2020) (e.g., ROS or calcium levels, even superoxide dismutase activity) can be easily achieved if the fit to cellular viability and *Bcl-2* promoter activity is acceptable (Figs. 1f and 4e) (Chong et al., 2014; Görlach et al., 2015). Therefore, our model closely aligns with the experimental data from Li et al. (2020) and can be used to make testable predictions.

The bistable system allows co-existence of two stable steady states (Spencer and Sorger, 2011). Bistability can be used to explain the binary decisions on cell fate (survival or death) (Spencer and Sorger, 2011). A bistable system is insensitive to minor perturbations and exhibits "all-or-none" transitions. From our simulation, we argue that TFA-mediated bistable responses are robust to large parametric stochasticity. However, we further note that the deterministic threshold for survival vs. death (i.e., SN_2 in Fig. 3a) is highly variable. TFA enhances Bcl-2 production and overexpressed anti-apoptotic Bcl-2 counteracts pro-apoptotic effectors such as BH3-only members and activated Bax to overcome the barriers to apoptosis (i.e., moves beyond SN_2). The maximum barrier height is also positively correlated with the survival threshold. These properties collectively imply that even there is robust bistability at system level; cell fate after TFA-treatment might vary with large

variations in the survival threshold. This effect may partially explain the "gradient" pattern in TFA dose responses seen in Li et al. (2020) and may also shed light on the phenomenon of "fractional killing" (Roux et al., 2015).

Specifically, we found that the effects of nimodipine and TFA may be increased when used in combination. These synergistic effects may be a salient feature of the protective roles of combined TFA-nimodipine treatment against OGD/R. Notably, the synergy between TFA and nimodipine was time- and dose-dependent (Figs. 5c and 5d). At early time points, TFA and nimodipine showed consistent synergy. However, if the measurements were performed at later time points, the combined effects may shift from synergism to antagonism depending on the TFA and nimodipine doses. Optimal synergy has been achieved approximately at the bistable regions in TFA and nimodipine space irrespective of temporal dependence. A monostable domain far from the bistable regions will mitigate the synergistic effects or even lead to antagonism. These findings argue that bistability may augment the synergistic effects and that the optimal use of TFA and nimodipine may offer favorable synergy for protecting neuronal cells against OGD/R-induced apoptosis. Since nimodipine is a neuro-protective drug already used in clinical practice (Roine et al., 1990) and TFA is a phytochemical extracted from black tea, the synergy between these two compounds suggests a potentially promising strategy. The synergy between TFA and nimodipine may possibly be more effective against drug-induced side effects compared with parenteral edaravone and nimodipine co-treatment (Li et al., 2018).

In summary, we investigated the protective role of TFA in the mitochondria apoptotic pathway. TFA-mediated bistability displays both robust and variable features. The synergistic effects of TFA and nimodipine may provide crucial insight into neuronal protection against ischemia stroke.

Acknowledgments

This research was supported by the National Natural Science Foundation of China (Nos. 31971185 and 31800316), the Key Projects of Support Program for Outstanding Young Talents in Colleges and Universities of Anhui Province (Nos. gxyqZD2020031 and gxyq2018034), and the Key Project of the Education Department of Anhui Province, China (No. KJ2017A359).

We thank Dr. Liangliang ZHU (School of Life Sciences, the Province Key Laboratory of the Biodiversity Study and Ecology Conservation in Southwest Anhui, Anqing Normal University, Anhui, China) for critical reading of the manuscript.

Author contributions

Dan MU and Tingzhe SUN conceptualized the study, performed project administration, and acquired the funding; Dan MU, Huaguang QIN, and Tingzhe SUN developed the methodology and wrote the manuscript; Dan MU, Huaguang QIN, Mengjie JIAO, Shaogui HUA, and Tingzhe SUN validated the study, performed the data analysis and curation, and reviewed the draft; Tingzhe SUN supervised the study. All authors have read and agreed to the published version of the manuscript, and therefore, have full access to all the data in the study and take responsibility for the integrity of the data and the accuracy of the data analysis.

Compliance with ethics guidelines

Dan MU, Huaguang QIN, Mengjie JIAO, Shaogui HUA, and Tingzhe SUN declare that they have no conflict of interest.

This article does not contain any studies with human or animal subjects performed by any of the authors.

References

Albeck JG, Burke JM, Spencer SL, et al., 2008. Modeling a snap-action, variable-delay switch controlling extrinsic cell death. *PLoS Biol*, 6(12):2831-2852. https://doi.org/10.1371/journal.pbio.0060299

Bagci EZ, Vodovotz Y, Billiar TR, et al., 2006. Bistability in apoptosis: roles of Bax, Bcl-2, and mitochondrial permeability transition pores. *Biophys J*, 90(5):1546-1559. https://doi.org/10.1529/biophysj.105.068122

Chen C, Cui J, Lu HZ, et al., 2007. Modeling of the role of a Bax-activation switch in the mitochondrial apoptosis decision. *Biophys J*, 92(12):4304-4315. https://doi.org/10.1529/biophysj.106.099606

Chong SJF, Low ICC, Pervaiz S, 2014. Mitochondrial ROS and involvement of Bcl-2 as a mitochondrial ROS regulator. *Mitochondrion*, 19:39-48. https://doi.org/10.1016/j.mito.2014.06.002

Chong SJF, Marchi S, Petroni G, et al., 2020. Noncanonical cell fate regulation by Bcl-2 proteins. *Trends Cell Biol*, 30(7):537-555. https://doi.org/10.1016/j.tcb.2020.03.004

Coling DE, Yu KCY, Somand D, et al., 2003. Effect of SOD1 overexpression on age- and noise-related hearing loss. *Free Radic Biol Med*, 34(7):873-880. https://doi.org/10.1016/s0891-5849(02)01439-9

Cui J, Chen C, Lu HZ, et al., 2008. Two independent positive feedbacks and bistability in the Bcl-2 apoptotic switch. *PLoS ONE*, 3(1):e1469. https://doi.org/10.1371/journal.pone.0001469

Dejean LM, Martinez-Caballero S, Guo L, et al., 2005. Oligomeric Bax is a component of the putative cytochrome c release

channel MAC, mitochondrial apoptosis-induced channel. *Mol Biol Cell*, 16(5):2424-2432. https://doi.org/10.1091/mbc.E04-12-1111

Dhooge A, Govaerts W, Kuznetsov YA, 2003. MATCONT: a MATLAB package for numerical bifurcation analysis of ODEs. *ACM Trans Math Softw*, 29(2):141-164. https://doi.org/10.1145/779359.779362

Fitzgerald JB, Schoeberl B, Nielsen UB, et al., 2006. Systems biology and combination therapy in the quest for clinical efficacy. *Nat Chem Biol*, 2(9):458-466. https://doi.org/10.1038/nchembio817

Görlach A, Bertram K, Hudecova S, et al., 2015. Calcium and ROS: a mutual interplay. *Redox Biol*, 6:260-271. https://doi.org/10.1016/j.redox.2015.08.010

Ho KL, Harrington HA, 2010. Bistability in apoptosis by receptor clustering. *PLoS Comput Biol*, 6(10):e1000956. https://doi.org/10.1371/journal.pcbi.1000956

Jiang H, Zhang LJ, Kuo J, et al., 2005. Resveratrol-induced apoptotic death in human U251 glioma cells. *Mol Cancer Ther*, 4(4):554-561. https://doi.org/10.1158/1535-7163.MCT-04-0056

Keizer EM, Bastian B, Smith RW, et al., 2019. Extending the linear-noise approximation to biochemical systems influenced by intrinsic noise and slow lognormally distributed extrinsic noise. *Phys Rev E*, 99(5):052417. https://doi.org/10.1103/PhysRevE.99.052417

Koubi D, Jiang H, Zhang LJ, et al., 2005. Role of Bcl-2 family of proteins in mediating apoptotic death of PC12 cells exposed to oxygen and glucose deprivation. *Neurochem Int*, 46(1):73-81. https://doi.org/10.1016/j.neuint.2004.06.006

Legewie S, Blüthgen N, Herzel H, 2006. Mathematical modeling identifies inhibitors of apoptosis as mediators of positive feedback and bistability. *PLoS Comput Biol*, 2(9):e120. https://doi.org/10.1371/journal.pcbi.0020120

Legrand AJ, Konstantinou M, Goode EF, et al., 2019. The diversification of cell death and immunity: *Memento mori*. *Mol Cell*, 76(2):232-242. https://doi.org/10.1016/j.molcel.2019.09.006

Letai A, Bassik MC, Walensky LD, et al., 2002. Distinct BH3 domains either sensitize or activate mitochondrial apoptosis, serving as prototype cancer therapeutics. *Cancer Cell*, 2(3):183-192. https://doi.org/10.1016/S1535-6108(02)00127-7

Li LX, Yiin GS, Geraghty OC, et al., 2015. Incidence, outcome, risk factors, and long-term prognosis of cryptogenic transient ischaemic attack and ischaemic stroke: a population-based study. *Lancet Neurol*, 14(9):903-913. https://doi.org/10.1016/S1474-4422(15)00132-5

Li QJ, Ji ZL, Li K, 2018. Effect of combination of parenteral edaravone and nimodipine on ischemic cerebral injury following cerebral hemorrhage. *Trop J Pharm Res*, 17(5):955-960. https://doi.org/10.4314/tjpr.v17i5.27

Li Y, Shi J, Sun XT, et al., 2020. Theaflavic acid from black tea protects PC12 cells against ROS-mediated mitochondrial apoptosis induced by OGD/R via activating Nrf2/ARE signaling pathway. *J Nat Med*, 74:238-246. https://doi.org/10.1007/s11418-019-01333-4

Liu CQ, Zhou RX, Sun SG, 2004. Nimodipine modulates Bcl-2 and Bax mRNA expression after cerebral ischemia. *J Huazhong Univ Sci Technol Med Sci*, 24(2):170-172. https://doi.org/10.1007/BF02885421

Liu L, Huang WW, Wang JH, et al., 2017. Anthraquinone derivative exerted hormetic effect on the apoptosis in oxygen-glucose deprivation-induced PC12 cells via ERK and Akt activated Nrf2/HO-1 signaling pathway. *Chem Biol Interact*, 262:1-11. https://doi.org/10.1016/j.cbi.2016.12.001

Luo YG, Yang XF, Zhao ST, et al., 2013. Hydrogen sulfide prevents OGD/R-induced apoptosis via improving mitochondrial dysfunction and suppressing an ROS-mediated caspase-3 pathway in cortical neurons. *Neurochem Int*, 63(8):826-831. https://doi.org/10.1016/j.neuint.2013.06.004

Mehta SL, Manhas N, Raghubir R, 2007. Molecular targets in cerebral ischemia for developing novel therapeutics. *Brain Res Rev*, 54(1):34-66. https://doi.org/10.1016/j.brainresrev.2006.11.003

Niture SK, Jaiswal AK, 2012. Nrf2 protein up-regulates antiapoptotic protein Bcl-2 and prevents cellular apoptosis. *J Biol Chem*, 287(13):9873-9886. https://doi.org/10.1074/jbc.M111.312694

Pellegrini-Giampietro DE, Mannaioni G, Bagetta G, 2009. Post-ischemic brain damage: the endocannabinoid system in the mechanisms of neuronal death. *FEBS J*, 276(1):2-12. https://doi.org/10.1111/j.1742-4658.2008.06765.x

Roine RO, Kaste M, Kinnunen A, et al., 1990. Nimodipine after resuscitation from out-of-hospital ventricular fibrillation: a placebo-controlled, double-blind, randomized trial. *JAMA*, 264(24):3171-3177. https://doi.org/10.1001/jama.1990.03450240073043

Roux J, Hafner M, Bandara S, et al., 2015. Fractional killing arises from cell-to-cell variability in overcoming a caspase activity threshold. *Mol Syst Biol*, 11(5):803. https://doi.org/10.15252/msb.20145584

Saito A, Maier CM, Narasimhan P, et al., 2005. Oxidative stress and neuronal death/survival signaling in cerebral ischemia. *Mol Neurobiol*, 31(1-3):105-116. https://doi.org/10.1385/MN:31:1-3:105

Seidman MD, 2000. Effects of dietary restriction and antioxidants on presbyacusis. *Laryngoscope*, 110(5):727-738. https://doi.org/10.1097/00005537-200005000-00003

Seidman MD, Khan MJ, Bai U, et al., 2000. Biologic activity of mitochondrial metabolites on aging and age-related hearing loss. *Am J Otol*, 21(2):161-167. https://doi.org/10.1016/s0196-0709(00)80003-4

Seidman MD, Khan MJ, Tang WX, et al., 2002. Influence of lecithin on mitochondrial DNA and age-related hearing loss. *Otolaryngol Head Neck Surg*, 127(3):138-144. https://doi.org/10.1067/mhn.2002.127627

Seidman MD, Ahmad N, Joshi D, et al., 2004. Age-related hearing loss and its association with reactive oxygen species and mitochondrial DNA damage. *Acta Otolaryngol Suppl*, (552):16-24. https://doi.org/10.1080/03655230410017823

Spencer SL, Sorger PK, 2011. Measuring and modeling

apoptosis in single cells. *Cell*, 144(6):926-939. https://doi.org/10.1016/j.cell.2011.03.002

Straetemans R, O'Brien T, Wouters L, et al., 2005. Design and analysis of drug combination experiments. *Biom J*, 47(3): 299-308. https://doi.org/10.1002/bimj.200410124

Sun TZ, Chen C, Wu YY, et al., 2009. Modeling the role of p53 pulses in DNA damage-induced cell death decision. *BMC Bioinformatics*, 10:190. https://doi.org/10.1186/1471-2105-10-190

Sun TZ, Lin XZ, Wei YN, et al., 2010. Evaluating bistability of Bax activation switch. *FEBS Lett*, 584(5):954-960. https://doi.org/10.1016/j.febslet.2010.01.034

Thompson JW, Narayanan SV, Perez-Pinzon MA, 2012. Redox signaling pathways involved in neuronal ischemic preconditioning. *Curr Neuropharmacol*, 10(4):354-369. https://doi.org/10.2174/157015912804143577

Tian TH, Burrage K, 2006. Stochastic models for regulatory networks of the genetic toggle switch. *Proc Natl Acad Sci USA*, 103(22):8372-8377. https://doi.org/10.1073/pnas.0507818103

Tsujimoto Y, 2003. Cell death regulation by the Bcl-2 protein family in the mitochondria. *J Cell Physiol*, 195(2):158-167. https://doi.org/10.1002/jcp.10254

Tyson JJ, Chen KC, Novak B, 2003. Sniffers, buzzers, toggles and blinkers: dynamics of regulatory and signaling pathways in the cell. *Curr Opin Cell Biol*, 15(2):221-231. https://doi.org/10.1016/S0955-0674(03)00017-6

Willis SN, Adams JM, 2005. Life in the balance: how BH3-only proteins induce apoptosis. *Curr Opin Cell Biol*, 17(6): 617-625. https://doi.org/10.1016/j.ceb.2005.10.001

Yang CJ, Hawkins KE, Doré S, et al., 2019. Neuroinflammatory mechanisms of blood-brain barrier damage in ischemic stroke. *Am J Physiol Cell Physiol*, 316(2):C135-C153. https://doi.org/10.1152/ajpcell.00136.2018

Yin ZY, Qi H, Liu LL, et al., 2017. The optimal regulation mode of Bcl-2 apoptotic switch revealed by bistability analysis. *Biosystems*, 162:44-52. https://doi.org/10.1016/j.biosystems.2017.09.011

Youle RJ, Strasser A, 2008. The BCL-2 protein family: Opposing activities that mediate cell death. *Nat Rev Mol Cell Biol*, 9(1):47-59. https://doi.org/10.1038/nrm2308

Supplementary information

Figs. S1 and S2; Tables S1–S3